Received: 8 October 2019 | Revised: 17 April 2020 | Accepted: 17 June 2020

DOI: 10.1002/suco.201900409

fib CEB-FIP WILEY

TECHNICAL PAPER

Flexural capacity of steel-FCB bar-reinforced coral concrete beams

Lei Wang[1,2] | **Zhaoping Song**[1] | **Changshi Huang**[1] | **Linjian Ma**[3] | **Feng Fu**[4,1]

[1]College of Civil Engineering and Architecture Engineering, Guilin University of Technology, Guilin, China

[2]Guangxi Beibu Gulf Engineering Research Center for Green Marine Materials, Guilin, China

[3]State Key Laboratory of Disaster Prevention and Mitigation of Explosion and Impact, Army Engineering University of PLA, Nanjing, China

[4]School of Mathematics, Computer Science and Engineering, City, University of London, London, UK

Correspondence
Feng Fu, School of Mathematics, Computer Science and Engineering, City, University of London, London, EC1V 0HB UK.
Email: cenffu@yahoo.co.uk

Funding information
Innovation-driven Development Project, Grant/Award Number: AA18242007-5; High-Level Innovation Team in Colleges and Universities and Excellence Scholar Program, Grant/Award Number: 201738-2; National Natural Science Foundation of China, Grant/Award Number: 51868014

Abstract

Steel-fiber composite bar (SFCB) is a new technique with steel core embedded into the fiber-reinforced polymer (FRP) bars, which solve the shortcomings of poor ductility and low stiffness of FRP-reinforced concrete members. Based on the experimental study, flexural behavior of a new type concrete, SFCB bars-reinforced coral concrete beams, is investigated. The deflection, failure mode, tensile strain, and ultimate flexural capacity of this new type of concrete beam are studied in detail through a series four-points bending tests. The results show that the failure process of SFCB-reinforced coral concrete beam can be divided into three main stages: elastic, cracking, and failure. Because exterior layer of SFCB bar is able to continue to withstand tensile stress after its steel core yield, hence, the flexural rigidity and flexural capacity of the beams both increase. The flexural stiffness of SFCB bars-reinforced coral concrete beams is also increased, and the load-deflection relation is more or less nonlinear. By using SFCB bars, the stiffness of the beams can be increased by about 20%. However, under high stress state, the relative slip between the carbon fiber and the concrete as well as that between the steel core and the carbon fiber cause tensile stress loss which weakened the flexural resistance of the SFCB bar-reinforced coral concrete beam. The bonding performance between the round surface steel core and the carbon fiber is obviously weaker than that of the threaded surface steel core, and the steel core slip is more likely to occur under the higher tensile stress. When Using ACI440.1R-15 and GB50608-2010 to calculate the flexural capacity of the SFCB beams, the ratios of the theoretical value and the measured value from tests are 1.07 and 1.12, respectively. By introducing two new factors k_1 and k_2, a formula was developed through modification of the existing ones from ACI440.1R-15 and GB50608-2010 to calculate

Discussion on this paper must be submitted within two months of the print publication. The discussion will then be published in print, along with the authors' closure, if any, approximately nine months after the print publication.

the ultimate flexural capacity of SFCB bar reinforced concrete beam which agrees as high as 93–99% with the experimental results.

KEYWORDS

coral concrete, deflection, flexural capacity, FRP, SFCB

1 | INTRODUCTION

The research[1,2] shows that, coral aggregates as coarse or fine aggregates can achieve a compressive strength of 20–50 MPa. Some initial comparative studies to common concrete have been made by the authors, it is found that coral concrete has the characteristics of early strength and rapid hardening. Its 28d cube compressive strength is similar to that of ordinary concrete, so as well the elastic modulus which is slightly lower than that of ordinary aggregate concrete with the same concrete strength grade, but not much. With proper preparation method, coral concrete has good engineering properties and can meet all kinds of engineering requirements.[1,3] Therefore, if they are used as building materials can greatly reduce the production and transportation costs of construction in remote island reef in coastal area. Therefore, it is a cost effective and environmental friendly option for construction projects in coastal area.[4,5,6] Problems of steel corrosion caused by a large amount of salt contained in coral concrete are reported in relevant research.[7,8,9] Fiber-reinforced polymer (FRP) bar is widely used in construction projects due to its excellent corrosion resistance, it has been widely used in hot and humid marine environment. However, due to the lower elastic modulus and unique bonding characteristics of FRP bars, FRP bars-reinforced concrete beams exhibit large deformation and small stiffness. In addition, the load-deflection curve increases linearly. There is no obvious yielding stage, and the component failure presents brittle characteristics. Such shortcomings become barriers for its engineering applications.[10,11,12]

A newly developed steel fiber composite bar (SFCB) provides a new way to solve the shortcomings of poor ductility and low stiffness of FRP-reinforced concrete members. In 1997, Tan KH[13] took the lead in the use of aramid fiber-reinforced polymer steel composite bars as the main tensile reinforcement of concrete beams. After that, Aiello[14] and Lau[15] performed preliminary study on the SFCB bars. Hao[16] and Ou et al.[17] studied the mechanical properties of steel-glass fiber reinforced polymer (GFRP). Wu Zhishen,[18] Ou,[19] Wu Gang,[20] and Dong et al.[21] stated that due to the introduction of steel core, the elastic modulus of SFCB bars is effectively improved, and the stress–strain relationship curve exhibit obvious yield point, and the steel core is more stable after yielding. Therefore, this new type of bars exhibits good ductility, shear resistance, and excellent corrosion resistance, and can reduce material costs. Different to normal FRP bars, the SFCB exhibit good ductility, therefore they are failure mode are more predictable, hence more stable and reliable compared to the conventional FRP bars. For this type of bars, the ratio of steel to FRP material directly determines the stress–strain characteristics of SFCB bars, as well as deflection, ultimate flexural capacity and failure mode of SFCB bars reinforced concrete beams.

The research in coral concrete is still very limited with only limited literature is available.[22,23,24] The substitution of SFCB bars with good ductility, high strength, and corrosion resistance for rebars or pure FRP bars in the construction of the island can effectively solve the problem of corrosion caused by high salinity of coral concrete and the problem of brittle damage caused by bending members. The combination of SFCB and coral concrete can effectively improve the service life and bending stiffness of coral concrete members. Due to the particular characteristic of coral concrete material and its application environment, no reports on the research of SFCB bar-reinforced coral concrete structure have been made so far. The effect of SFCB on the mechanical properties of coral concrete beams is not clear.

Therefore, in this article, the four-points bending tests of SFCB bars-reinforced coral concrete beams were

FIGURE 1 SFCB bars. SFCB, steel-fiber composite bar

TABLE 1 Specifications of bars and their mechanical properties

Type of bar	Diameter (mm)	Actual diameter (mm)	Internal core shape	Bar height (mm)	Bar width (mm)	Bar spacing (mm)	Elastic modulus after yielding (GPa)	Yield strength (MPa)	Extreme strength (MPa)	Elastic modulus (GPa)
SFCB bar	12(6)	11.45	Threaded	0.50	8.68	10.98	40.9	167.8	920.56	126.9
	14(6)	14.08	Glossy	1.13	6.83	10.15	75.9	173.2	1,073.8	132.6
	14(8)	14.10	Threaded	0.68	11.00	13.50	57.6	233.7	858.4	136.0
	16(10)	15.80	Threaded	0.53	13.13	15.25	62.5	263.5	881.0	142.3
Steel rebar	14	—	—	0.71	2.10	7.82	—	429.0	608.0	200.0

Note: The diameter of the SFCB bar in brackets is expressed as 12(6), the diameter of SFCB bar is 12 mm, and the diameter of inner steel core is 6 mm.
Abbreviation: SFCB, steel-fiber composite bar.

FIGURE 2 Coral debris

FIGURE 3 Coral sand

performed, the flexural capacity and failure modes of SFCB-reinforced coral concrete beams are studied. The effects of properties of longitudinal SFCB reinforcement, coral concrete strength, percentage of SFCB reinforcement, and the steel core shape on the structural behavior of the coral concrete beams were studied. The calculation formula of the flexural capacity of SFCB-reinforced coral concrete beams is developed.

2 | TEST PROGRAMS

2.1 | Test specimens

As it shown in Figure 1, four types of SFCB bars were used in the tests, they are manufactured by China's

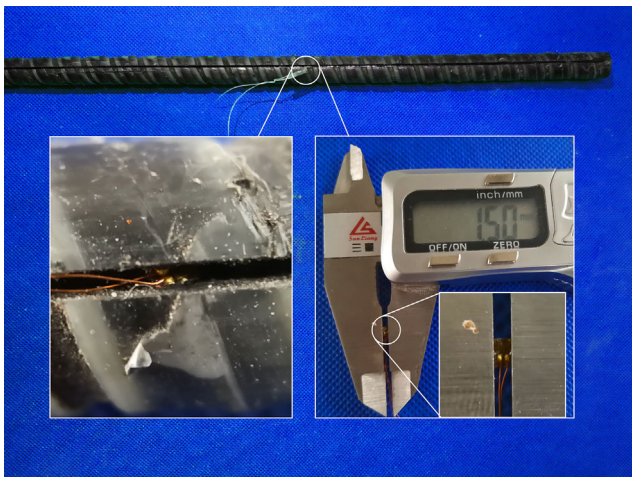

FIGURE 4 Groove of SFCB. SFCB, steel-fiber composite bar

FIGURE 5 Tensile failure mode of SFCB bars. SFCB, steel-fiber composite bar

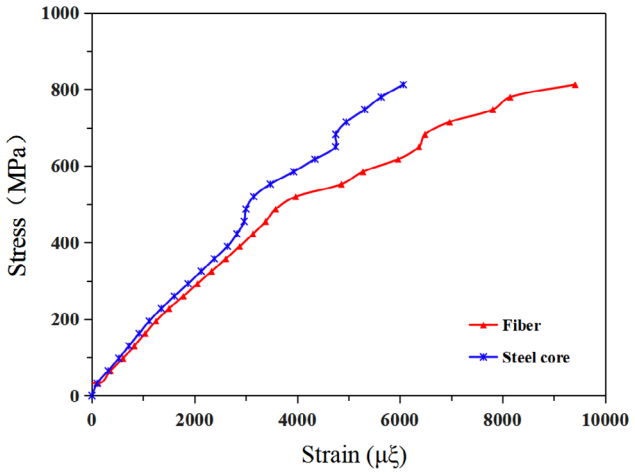

FIGURE 6 SFCB-14 (6) monotonically stretched stress–strain curve of fiber/steel core. SFCB, steel-fiber composite bar

intelligent fiber composite reinforcement Nantong Co., Ltd. Their mechanical properties are shown in Table 1; 14 mm diameter HRB400 steel bar was used as the core of the SFCB bars. Figures 2 and 3 show the coarse aggregate: Corrugated coral debris and fine aggregate coral sand. Grade PO 42.5 Portland cement was used. Artificially prepared seawater with a concentration of 3.5% in the casting. In addition, water reducer with about 20% of polycarboxylate superplasticizer is added into the mix, which accounts 0.1% of cement mix. Three different strengths coral concrete were achieved. The detailed mix

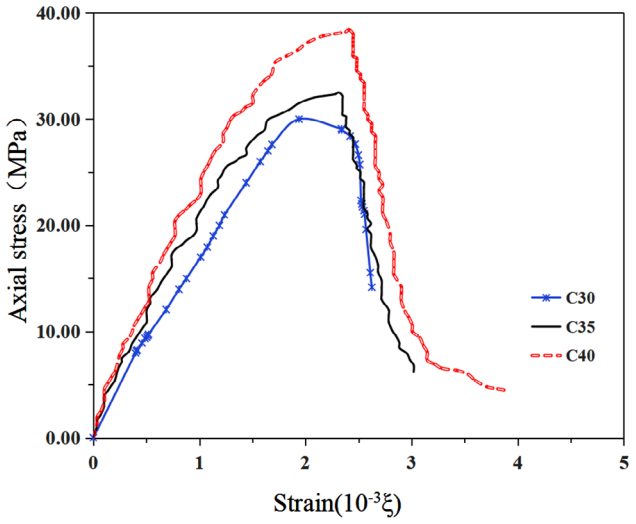

FIGURE 7 Stress–strain curve of coral concrete

design and mechanical properties of each composition are shown in Table 2.

The failure pattern of SFCB bars in tensile test as showed in Figure 5, and the failure mode is either the fracture of steel core or the concentrated fracture of wrapped fiber drops sharply. Figure 6 shows the stress–strain curve of the steel core and fiber of SFCB-14 (6) composite reinforcement under tensile load, which is slotted in the middle of the tensile specimen and measured by fiber bragg grating. It can be seen from Figure 6 that before the steel core yields, it is well bonded with the outer fiber, due to smaller stiffness of fiber than the steel core, fiber strain is slightly larger than that of the steel core, but the difference is not large. When the steel core yields, the plastic deformation of the steel core increases, which destroys the bond between the steel core and the fiber, resulting in the local sliding of the steel core and the fiber layer, the results show that the fiber strain after yield is much larger than that of steel core, and the steel core shows stress lag phenomenon. Figure 7 shows the axial stress–strain curve of coral concrete measured by strain gauge. The axial stress–strain curve of coral concrete is similar to ordinary concrete, but when it reaches the peak value of stress, it shows a rapid decrease of strain and sudden brittle failure due to the influence of porous brittleness of coral aggregate.

In order to study the mechanical properties and damage characteristics of the steel core, fiber and coral concrete materials bending test beams with different reinforcement rate, steel core content and strength of coral concrete were performed. The size of the test beam is 120 mm × 250 mm × 2,400 mm, and a total of seven groups are casted. Among them, 12 are SFCB-reinforced coral concrete beams and 2 are normal steel-reinforced

TABLE 2 Mix proportion and mechanical properties of coral concrete

Concrete strength (water-cement ratio)	Cement (kg/m^3)	Coral (kg/m^3)	Coral sand (kg/m^3)	Sea water (kg/m^3)	Water-reducing agent (kg/m^3)	Cube compressive strength (MPa)	Axis compression strength (MPa)	Cracking tensile strength (MPa)	Elastic modulus (GPa)
C30 (0.37)	530	823	760	196	0.53	34.8	29.6	1.91	27.1
C35 (0.33)	555	823	760	183	0.555	37.7	32.5	2.10	28.8
C40 (0.28)	580	823	760	163	0.58	44.0	38.4	2.36	31.6

TABLE 3 Basic parameters table of specimen beam

Test beam number	$b \times h \times l$ (mm)	l_0 (mm)	Tensile reinforcement (beam)	Lace bars (beam)	Stirrup spacing	Equivalent reinforced ratio, %
C30-F14(8)-1,2	120 × 250 × 2,400	2,100	2F14(8)	2Φ6CFRP	Φ6CFRP@80	0.92
C35-F12(6)-1,2	120 × 250 × 2,400	2,100	2F12(6)	2Φ6CFRP	Φ6CFRP@80	0.72
C35-F14(6)-1,2	120 × 250 × 2,400	2,100	2F14(6)	2Φ6CFRP	Φ6CFRP@80	1.04
C35-F14(8)-1,2	120 × 250 × 2,400	2,100	2F14(8)	2Φ6CFRP	Φ6CFRP@80	0.92
C35-F16(10)-1,2	120 × 250 × 2,400	2,100	2F16(10)	2Φ6CFRP	Φ6CFRP@80	1.14
C35-S14-1,2	120 × 250 × 2,400	2,100	2S14	2Φ6CFRP	Φ6CFRP@80	1.18
C40-F14(8)-1,2	120 × 250 × 2,400	2,100	2F14(8)	2Φ6CFRP	Φ6CFRP@80	0.92

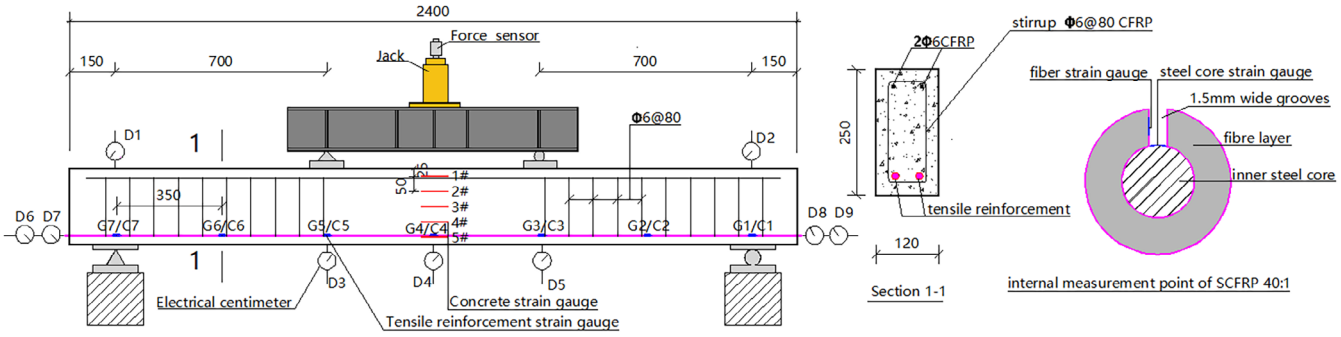

FIGURE 8 Diagram of instrumentations and loading device

coral concrete beams as reference beams. Single layer of longitudinal reinforcement is used in each beam with 5 mm length extended out at the beam end to facilitate monitor the relative slip between the longitudinal bar and the coral concrete. The CFRP stirrups with Φ6@80 are arranged in the shear zone. The CFRP bars with a diameter of 6 mm are used for the lace bars. The concrete cover is 25 mm, the RC details are shown in Table 3. The test beams are numbered as M-Rd(ds)-1 or 2, where M is the strength of the coral concrete, R is the type of the reinforcement (F stands for SFCB, S stands for steel), d is the diameter of the reinforcement, and d_s is the diameter of the steel core. 1 or 2 is the number of the same test beam. In the table, the "equivalent reinforcement ratio" of the SFCB-reinforced coral concrete beam is obtained by converting the SFCB bars into the equivalent area of the FRP bars according to the principle of equal fiber strength, the formula to calculate the equivalent reinforcement ratio of SFCB bars is $\rho_e = \frac{A_s f_y + A_f f_{fd}}{f_{fd} \cdot b \cdot h_0}$. The reinforcement ratio of the reinforced concrete beam is the actual reinforcement ratio of the steel bars.

2.2 | Instrumentation and loading process

As shown in Figure 8, four-point bending tests were performed. An increment of 1 kN was adopted before

cracking. After cracking, increment changed to 3 kN, and the loading increment increased until 90% of the ultimate load was approached.

The tensile strain of the longitudinal reinforcement, the strain of coral concrete and the deflection of beam, the development of cracks, the slip of the main longitudinal reinforcement were monitored during the tests using similar instrumentation of reference.[30–33,34] The strain measurement of the SFCB bars was obviously more difficult than that of the single material bars. In order to measure the strain of the steel core and the carbon fiber, in this test, a groove with a width of 1.5 mm is engraved on the surface of the SFCB bars up to the surface of the steel core, and on the surface of the steel core and the side of the groove, a strain gauge was mounted, as shown in Figures 4 and 8. There are seven measuring points in the SFCB bars, which are located in the mid span of the beam, the loading point, the 1/2 of shear bending zone and the support. The surface of the test beam was also mounted with strain gauges from the bottom to the top to measure the concrete strain at location 25, 75, 125, 175, 225 mm across the section. Five dial gauges were installed at mid span, loading point, and support to measure the deformation of the test beam under different load conditions. Dial gauges were also placed at both ends of the test beam at the location of the extended SFCB bars. Another two dial gauges were placed set on the concrete surface. These four gauges were used to measure the relative slip between the SFCB bar and the concrete.

3 | TEST RESULT ANALYSIS

3.1 | Failure modes

The failure modes of beams are key in resisting global collapse of a building.[35,36,37] Each specimen are shown in Figure 9 and Table 4. The equivalent fiber reinforcement ratio of all the test beams in this article is greater than required reinforcement ratio in the design, and there is no fracture of the main tensile reinforcement observed before the concrete in the compression zone is destroyed. The failure modes of most of the test beams are similar to ordinary steel reinforced concrete. As the bending moment increases, the cracks in the tension zone are observed continuously, and after the component undergoes large deflection, the concrete in the compression zone crushed. However, due to the influence of different types of materials, the experimental phenomena and failure modes of SFCB-reinforced coral concrete beams still have obvious differences with the normal steel-reinforced concrete beams. This is because the bonding properties of SFCB bars and coral concrete are weaker than that of steel bars, and the lower modulus of elasticity results in the crack width, spacing, and deflection of the SFCB bar reinforce coral concrete beam under the same load conditions are greater than that of steel reinforced concrete beam. With the increase of the reinforcement ratio and the steel content of SFCB, the crack width and spacing of SFCB-reinforced coral concrete beams are reduced, and the bending stiffness is also significantly increased.

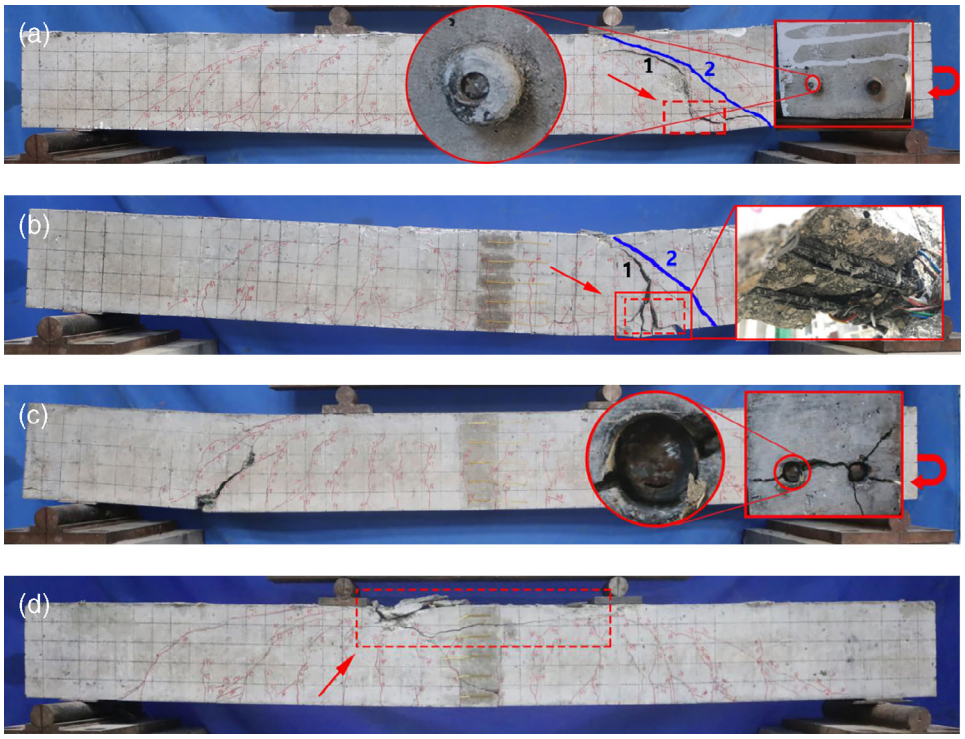

FIGURE 9 Crack patterns and failure modes of beams

TABLE 4 Bending damage feature parameters of specimen beams

Test beam number	ρ_{sf-s} (%)	A_{sf} (mm^2)	A_{sf-s} (mm^2)	A_{sf-f} (mm^2)	P_{cr} (kN)	F_u (kN)	Failure mode
C30-F14(8)-1	32.68	307.8	100.6	207.2	9	99	Concrete crushed
C30-F14(8)-2	32.68	307.8	100.6	207.2	6	98.7	Concrete crushed
C35-S14-1	—	—	307.8	—	10	82	Concrete crushed(rebar yields)
C35-S14-2	—	—	307.8	—	15	85	Concrete crushed(rebar yields)
C35-F12(6)-1	25.02	226.2	56.6	169.6	9	85.5	Bend section failure(fragmentation of fiber)
C35-F12(6)-2	25.02	226.2	56.6	169.6	6	95.5	Concrete crushed
C35-F14(6)-1	18.39	307.8	56.6	251.2	6	93	Glue break(steel core slip)
C35-F14(6)-2	18.39	307.8	56.6	251.2	6	120.6	Glue break(steel core slip)
C35-F14(8)-1	32.68	307.8	100.6	207.2	6	102	Concrete crushed
C35-F14(8)-2	32.68	307.8	100.6	207.2	9	107	Concrete crushed
C35-F16(10)-1	39.04	402.2	157	245.2	9	120	Glue break(longitudinal slip)
C35-F16(10)-2	39.04	402.2	157	245.2	6	109.6	Concrete crushed
C40-F14(8)-1	32.68	307.8	100.6	207.2	9	116.6	Concrete crushed
C40-F14(8)-2	32.68	307.8	100.6	207.2	9	100.6	Concrete crushed

Note: F represents SFCB bar beams, S represents rebar beams, in which, except for C35-F12(6), the inner steel core of the SFCB bars are threaded. ρ_{sf-s} represents the inner steel core content of SFCB bar, A_{sf} represents the total area of the SFCB bar, A_{sf-s} for inner steel core area, A_{sf-f} for fiber area, P_{cr} for cracked load, and F_u for ultimate load.
Abbreviation: SFCB, steel-fiber composite bar.

TABLE 5 Compatibility coefficient between inner steel core and fiber

	Glossy of inner steel core		Threaded of inner steel core	
Assignment definition	Before yield	After yield	Before yield	After yield
k_1	0.85–0.95	0.7–0.9	0.9–1.0	0.85–0.95

In addition, unlike the normal reinforced concrete beam, there are a large number of cracks in the bottom of the SFCB reinforced beam along the bars. Because the SFCB bar can still bear large tensile stress after the steel core yields, under the high stress state, the stress difference of SFCB bar at the crack location and between the cracks is larger. This is the main reason for the longitudinal cracking along the bars,[20] especially at the junction of the pure bending zone and shear bending zone, and the anchorage zone at the beam end.

It is necessary to pay special attention to the fact that the bond capacity between steel core, carbon fiber as well as SFCB and coral concrete have significant effects on the working performance and failure mode of SFCB-reinforced coral concrete beams. The relative slip between the carbon fiber and the concrete, the steel core and the carbon fiber of some of the test beams caused the flexural capacity of the beams to be greatly weakened and caused some abnormal damages.

The slip of between the SFCB bars and the concrete or between the steel core and exterior layer of FRP will cause the tensile stress loss, and the loss will gradually increase from the middle to the ends; the damage position can be seen in Figure 9a,b. It can be seen that, the internal main tensile stress loss is not as serious as the beam end; however, this zone is still subjected to a large bending moment. The failure is caused by the combination of large bending moment and shear force. The failure mode is quite different from the bending and shear failure of ordinary reinforced concrete members. The crack pattern is different from the crack development in common bending and shearing zones (as it shown in Figure 9a,b). For the test beam C35-F16(10) -1, due to the large diameter of the SFCB bars, the relative thickness of the concrete cover (c/d) is small, and the radial stress caused by the adhesion of the SFCB bar to the beam end causes crack. It can also be noticed that, The SFCB tended to slip, but its steel core did not slip, as shown in Figure 9c.

For the test beam without obvious slip, due to the linear elastic characteristics of the fiber, the deformation of outer carbon fiber of the SFCB bar after unloading is reduced, and the residual deflection of the test beam after bending failure is smaller than that of the steel-reinforced concrete beam; in addition, due to the lower strength of

coral aggregate, the brittleness of coral concrete under compression is more obvious than that of ordinary concrete. When the test beam is damaged by the coral concrete in the compression zone, there will be long cracks, as shown in Figure 9(d).

3.2 | Load-deflection relation

The load-deflection curve of the beam is shown in Figure 10. It can be roughly divided into three working phases: (a) The elastic working phase before the cracking, when the initial load is small, and the load-deflection curve of the test beam changes linearly. Because the concrete in the tension zone is involved in the work, the bending stiffness of each test beam is not much different, and it is basically in the elastic working state; (b) In the working stage with cracks, as the load increases, the concrete in the tension zone cracks. The tensile stress is mainly provided by the SFCB bars. The tensile strength of the beam is significantly reduced, and the first inflection point occurs. After that, the growth speed of the mid-span deflection is accelerated. At the same time, due to the different types and ratio of reinforcement, the deflection of the test beams began to show significant differences; (c) After the yielding of the steel bars, the deflection of the steel reinforced concrete beams was not significantly increased after the load was applied. It grows rapidly and then breaks. For the SFCB reinforced coral concrete beam, after the inner steel core of the SFCB bar yields, the outer carbon fiber can continue to bear the increased tensile stress, but the increase speed of the mid-span deflection is obviously accelerated. When failure occurred, slips of the SFCB bars were evident.

It should be noted that the load-deflection curves of C30-F14(8)-1 and C35-F14(8)-1 are very similar at the yielding stage due to the slip of SFCB bars which cause a so-called "false yield." Under the same load conditions, the deflection of the beam becomes smaller with the increase of the reinforcement ratio (the rigidity of the carbon fiber is converted into the equivalent area of the steel bar), and the deflection of the C35-S14-1 in the reinforced concrete beam is the smallest. C35-F12(6)-1 has the largest deflection, and the latter is about 2 to 4 times that of the former. Increasing the strength of the coral concrete is beneficial to reduce the deflection of the beam. Under the same reinforcement condition, the maximum mid-span deflection of the C40-F14(8)-1 26% and 15%. Less than that of C30-F14(8)-1, C35-F14(8)-1. It should be noted that the stiffness of the beam is improved with the increase of the steel content of the SFCB bars. Under the same load, the deflection of C35-F14(8)-1 is reduced by about 20% compared with C35-F14(6)-1. In addition, although the test beam did not show a significant yield stage, the load-deflection curve began to exhibit a double-fold line characteristic compared to the normal FRP reinforced beam.

3.3 | Load-longitudinal bar strain relation

As it shown in Figure. 11, the load-longitudinal SFCB bar strain curve of the beam can be divided into three stress stages:

1. Before bottom concrete cracking, concrete cracking in tension zone, the concrete is working together with SFCB bars, both in elastic stage the steel core and the fiber strain cooperate with each other and increase linearly with the load.

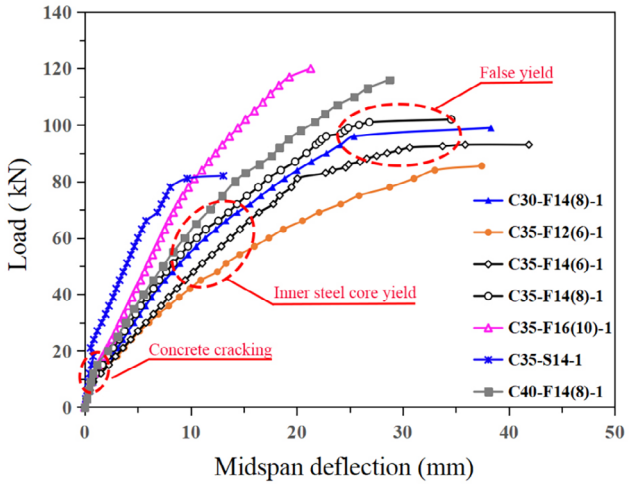

FIGURE 10 Load-midspan deflection curves

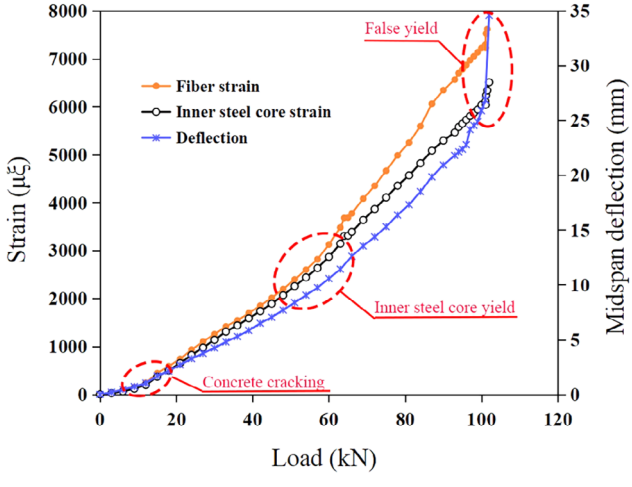

FIGURE 11 Load-midspan deflection and midspan strain curve of C35-F14(8)-1

2. Concrete cracking, SFCB works on its own. The tensile stress is mainly borne by the main tensile reinforcement. The strain of the SFCB bar is greatly increased. The strain of the outer carbon fiber is slightly larger than that of the steel core at the same measuring point, but their slope is the same, indicating that the steel core is bonded to the outer carbon fiber during this stress period.
3. As the load increases, the steel core of SFCB bar yields. After that, the beam can continue to resist the increasing load. The new tensile stress is mainly borne by the outer carbon fiber. The stress–strain of carbon fiber shows an inflection point after the steel core yields, and it begins to exhibit certain nonlinear characteristics. The higher the steel content, the more obvious the nonlinear characteristics. During the test, the strain value of the round steel core showed significant difference to the outer carbon fiber at yield stage. The larger the difference is, the larger the slip between the steel core and the carbon fiber observed. When the SFCB reinforced beam is close to failure, the deflection increase speed is obviously faster than that of the strain of SFCB bars, indicating that the slip between SFCB bars and the coral concrete slip, and the integrity of the beam is destroyed.

4 | CALCULATION OF THE FLEXURAL CAPACITY

At present, there are few studies on the flexural capacity of SFCB-reinforced concrete beams. The calculation of relevant flexural capacity can only be found from the existing steel or fiber reinforced concrete structural members. The calculation formula in ACI440.1R-15[25] and GB50608-2010.[26] GB50010-2010[27] are used to calculate the flexural capacity of SFCB-reinforced coral concrete beam and compares it with the measured value from the test. The calculation assumes four assumptions:

1. Plane sections remain plan
2. The tensile strength of coral concrete after cracking is ignored
3. The stress–strain relationship of coral-concrete is similar to lightweight aggregate concrete.[28]
4. The stress- strain curve of SFCB bar is linear before its yield

First of all, it is necessary to judge whether the reinforcement of the SFCB-reinforced beam is in the range of suitable amount. In this article, the SFCB bars is converted into CFRP bars according to the principle of equal fiber strength, and compared with the equilibrium reinforcement ratio:

$$\rho_{fb} = \alpha_1 \beta_1 f_c E_f \varepsilon_{cu} / \left[f_{fu} \left(E_f \varepsilon_{cu} + f_{fu} \right) \right] \tag{1}$$

$$\rho_f = A_{f1} / b h_{of} \tag{2}$$

From above formula, it can be seen that, all $\rho_f > \rho_{fb}$ and greater than $1.5\rho_{fb}$, so the amount of the reinforcement is suitable.

4.1 | ACI440.1R-15

According to equilibrium condition, and ACI440.1R-15,[25] the flexural capacity of SFCB-reinforced coral concrete beam are developed here.

$$f_{fu} = C_E f^*_{fu}, \tag{3}$$

where f_{fu} is the design tensile strength of FRP bars, C_E is the environment factor of CFRP bars, taking as 0.9 under marine environment.

The remaining symbol is same as ACI 440.1R-15[25]

The compatibility relation

$$c/(d-c) = \varepsilon_{cu}/\varepsilon_f, \tag{4}$$

where c is the distance between the bottom of the beam to the neutral axis; d is the effective height of the beam.

The remaining symbol is same as ACI440.1R-15[25]

Three grades of coral reef are used, so the concrete reduction factor are varied as following formula:

$$\beta_1 = 0.85 - 0.05(f_c - 28)/7. \tag{5}$$

When $\rho_f > \rho_{fb}$, the effective design stress f_f in cobordance to ACI440.1R-15[25] are:

$$f_f = \sqrt{0.25\left(A_s f_y / A_f + E_f \varepsilon_{cu}\right)^2 + \alpha_1 \left(\beta_1 f_c / \rho_f - A_s f_y / A_f\right) E_f \varepsilon_{cu}} - 0.5\left(A_s f_y / A_f + E_f \varepsilon_{cu}\right), \tag{6}$$

$$M_u = \left(\rho_f f_f + \rho_s f_y\right)\left[1 - 0.59\left(\rho_f f_f + \rho_s f_y\right)/f_c\right] b d^2, \tag{7}$$

$$F_{ACI,p} = M_u \times 6 / l_0 / 1000, \tag{8}$$

where f_f is effective design stress of equivalent FRP bar in tension zone, MPa; M_u is bending moment, N.m; $F_{ACI,p}$ is ultimate load, kN; l_0 is the span of the beam 2,100 mm;

And the remaining symbol is same as ACI440.1R-15[25] and ACI318-14.[29]

4.2 | GB50608-2010 and GB50010-2010

According to GB50608-2010[26] and GB50010-2010,[27] at failure,$\varepsilon_c = \varepsilon_{cu}$, $\varepsilon_{sfy} < \varepsilon_{sf}$

So the tensile strain of SFCB bar ε_{sf}:

$$\varepsilon_{sf} = \frac{\varepsilon_{cu}(h_0 - x_c)}{x_c}. \tag{9}$$

The overall area of SFCB bar is $A_{sf} = A_s + A_f$,

$$\sum N = 0$$

So,

$$\alpha_1\beta_1 f_c b x_c = A_{sf} f_{sf} = f_y A_s + \frac{\varepsilon_{cu}(h_0 - x_c)}{x_c} E_f A_f \tag{10}$$

$$x_c = \frac{-B \pm \sqrt{B^2 - 4AC}}{2A} \tag{11}$$

$$\sum M = 0$$

So,

$$M_u = \left(f_y A_s + \frac{\varepsilon_{cu}(h_0 - x_c)}{x_c} E_f A_f\right)\left(h_0 - \frac{x}{2}\right) \tag{12}$$

$$F_{GB,p} = M_u \times 6/l_0/1000 \tag{13}$$

Substituting the relevant material parameters of the beam into the above formula, the ultimate capacity of the SFCB reinforced beam can be obtained based on ACI440.1R-15[25] and GB50608-2010,[26] as shown in Table 7. It can be seen that both calculated values are significantly larger than the experimental values. The main reason is that the bonding performance and compatibility between SFCB bars and coral concrete is overestimated. It can be proved by experiments that different degrees of slip occur between SFCB bars and coral concrete in the latter stage of loading. The tensile stress loss of SFCB bars further reduces the flexural capacity. It does not take into account the steel core and carbon fiber slip of some SFCB bars. The tensile stress caused by the movement of the steel core was not fully considered. Therefore, in the calculation of the flexural capacity of SFCB-reinforced coral concrete beam, it is necessary to consider the reduction caused by the bond slip between the SFCB bars and the coral concrete as well as between SFCB fiber and steel core in the bars.

4.3 | A new modified formula

If we use k_1 to represent the compatibility between the steel core and the fiber, k_2 to represent the compatibility of SFCB bars and coral concrete. Due to the difference between the properties of steel and fiber materials, the compatibility of steel core and fiber under real stress conditions are not perfect. Under normal circumstances, the greater the stress, the worse the compatibility, especially in the stress stage after the steel core yields; In addition, it is also affected by factors such as the interface between the steel core and the fiber, the steel core material, and the steel core ratio of the SFCB bars.

The determination of the specific value of k_1 is extremely difficult. Under different stress levels, the bond performance between SFCB bars and coral concrete determines the value of k_2, which is mainly affected by factors such as the diameter of SFCB bars, the surface condition, the geometric parameters of the transverse bars on the surface of the bars, and the strength of the concrete. In our previous study,[38] The value of k_1 can only be determined from the tensile properties of the reinforcement, and the value of k_2 is determined from the experimental results of the bond between the SFCB reinforcement and coral concrete.

The actual stress–strain curve of the steel Core/fiber are given in Section 2.1 showing that the bond was destroyed due to the large plastic deformation of the steel core after yielding, the steel core shows a stress lag phenomenon, so k_1 can be determined from the tensile test of the reinforcement. And k_2 is similar to characteristic coefficient of bond between FRP bars and concrete in Chinese and American codes. Considering the bond between SFCB and coral concrete, it is mainly affected by the diameter, surface condition, surface of SFCB and concrete strength.

For example, ACI440.1R-15[25] considers the bonding characteristics of FRP bars and concrete and introduces the correction parameters k_b. However, its values are based on steel bars. When the bond strength of the bars is better than steel bars, the value is greater than 1, otherwise it is less than 1. It should be noted that k_2 has a significant effect on the value of k_1. If the bonding property between SFCB and concrete is poor or even slippage, the overall tensile stress of SFCB tends to decrease that is, the smaller the k_2 value, the relatively high value of k_1.

By introducing the compatibility coefficients k_1 and k_2, the flexural capacity of the SFCB bar test beam is modified as follows based on the US ACI440.1R-15[25] and the Chinese GB50608-2010[26]:

Introducing k_1 and k_2 into ACI440.1R-15 formula, we get:

$$f_{f,k}=\sqrt{0.25\left(\frac{k_1A_sf_y}{A_f}+E_f\varepsilon_{cu}\right)^2+\alpha_1\left(\frac{\beta_1f_c}{\rho_f}-\frac{k_1A_sf_y}{A_f}\right)E_f\varepsilon_{cu}}-0.5\left(\frac{k_1A_sf_y}{A_f}+E_f\varepsilon_{cu}\right) \quad (14)$$

$$M_{u,k}=k_2\left(\rho_ff_{f,k}+\rho_sf_y\right)\left[1-0.59\left(\rho_ff_{f,k}+\rho_sf_y\right)/f_c\right]bd^2. \quad (15)$$

Introducing k_1, and k_2 into GB50608-2010, we get:

$$\alpha_1\beta_1f_cbx_c=A_{sf}f_{sf}=k_1A_sf_y+\frac{\varepsilon_{cu}(h_0-x_c)}{x_c}E_fA_f \quad (16)$$

$$M_{u,k}=k_2\left(k_1A_sf_y+\frac{\varepsilon_{cu}(h_0-x_c)}{x_c}E_fA_f\right)\left(h_0-\frac{x}{2}\right). \quad (17)$$

In summary, the SFCB-reinforced concrete beams have the compatibility relationship between the steel core-fiber-concrete and their two interfaces, the compatibility is introduced through k_1 and k_2 coefficient, which is used to modify the formula of the flexural bearing capacity in the existing design guidelines. However, the factors affected by the compatibility are very complicated. Based on the experimental data and the related literature, the recommended range of values for k_1 and k_2 is given in Tables 5 and 6.

TABLE 6 Compatibility coefficient between SFCB bars and concrete

Assignment definition	Good bonding	Poor bonding
k_2	0.85–0.95	0.7–0.85

Abbreviation: SFCB, steel-fiber composite bar.

4.4 | Validation of the new modified formula

The calculated flexural capacities of the positive and negative bending moment based on the modified of formula

TABLE 7 Comparison of measured and calculated values of ultimate flexural capacity of test beams

		ACI 440.1R-15				GB50608-2010			
Test beam number	F_u (kN)	$F_{ACI,p}$	k_1	k_2	$F_{ACI,k}$	$F_{GB,p}$	k_1	k_2	$F_{GB,k}$
C30-F14(8)-1	99.0	104.9	0.90	0.85	88.0	108.4	0.90	0.85	91.4
C30-F14(8)-2	98.7	104.9	0.90	0.85	88.0	108.4	0.90	0.85	91.4
C35-F12(6)-1	85.5	97.6	0.88	0.86	83.2	104.0	0.88	0.86	88.8
C35-F12(6)-2	95.5	97.6	0.88	0.86	83.2	104.0	0.88	0.86	88.8
C35-F14(6)-1	93.0	110.2	0.70	0.92	99.4	118.0	0.70	0.92	107.2
C35-F14(6)-2	120.6	110.2	0.70	0.92	99.4	118.0	0.70	0.92	107.2
C35-F14(8)-1	102.0	109.4	0.90	0.88	95.1	114.7	0.90	0.88	100.1
C35-F14(8)-2	107.0	109.4	0.90	0.88	95.1	114.7	0.90	0.88	100.1
C35-F16(10)-1	120.0	121.9	0.93	0.87	104.8	125.3	0.93	0.87	108.1
C35-F16(10)-2	109.6	121.9	0.93	0.87	104.8	125.3	0.93	0.87	108.1
C40-F14(8)-1	116.6	117.4	0.90	0.90	104.5	126.6	0.90	0.90	113.1
C40-F14(8)-2	100.6	117.4	0.90	0.90	104.5	126.6	0.90	0.90	113.1

Note: F_u represents the measured ultimate load of SFCB test beams, kN; $F_{ACI,p}/F_{GB,p}$ represents the calculated ultimate load of SFCB test beams based on ACI440.1R-15/GB50608-2010; $F_{ACI,k}/F_{GB,k}$ represents the calculated ultimate load of SFCB test beams after considering the introduction of k_1, k_2 coefficient based on ACI440.1R-15/GB50608-2010. The average value of the calculated value and the measured value is 1.07, the *SD* is 0.07, and the coefficient of variation is 0.07(based on ACI440.1 R-15); the average value of the calculated value and the measured value is 1.12, the *SD* is 0.08, and the coefficient of variation is 0.07(based on GB50608-2010). After considering the introduction the synergistic coefficient of k_1 and k_2, the average value of the calculated value and the measured value is 0.93, the *SD* is 0.07, and the coefficient of variation is 0.09(based on ACI440.1R-15); the average value of the calculated value and the measured value is 0.99, the *SD* is 0.08, and the coefficient of variation is 0.08(based on GB50608-2010).

Abbreviation: SFCB, steel-fiber composite bar.

form China and the United States codes are shown in Table 7. It can be seen that, when using ACI440.1R-15 and GB50608-2010 to calculate the flexural capacity of the SFCB beams, the ratios of the theoretical value and the measured value from tests are 1.07 and 1.12, respectively.

It can be seen from Table 7 that considering the interface influence parameters of SFCB bars and coral concrete, SFCB steel cores and fibers, the calculated capacities are in good agreement with test results and has a certain safety reserve. The capacity based on the US ACI440.1R-15[25] is more conservative, and the one from of Chinese code is closer to the measured value.

5 | CONCLUSIONS

In this article, through experimental studies on the flexural behavior of SFCB bars-reinforced concrete beams, the influence of SFCB on the deflection, failure mode, tensile strain, and ultimate flexural capacity of SFCB-reinforced coral concrete beams is analyzed. Modified design formula based on ACI440.1R-15 and, GB50608-2010 are developed through the introduction of compatibility coefficient between core and fiber, bond coefficient SFCB bar and coral concrete, below conclusions are made:

1. When reinforcement ratio is greater than the equilibrium reinforcement ratio, the failure process of SFCB bar coral concrete beam is similar to that of steel-reinforced concrete beam. It can be divided into three stages: elastic, cracking, and damage; however, the relative slip between steel core and carbon fiber, as well as between carbon fiber and concrete will decrease the bending resistance and cause abnormal damage
2. After the steel core is yielded, the outer layer fiber of SFCB can continue to withstand tensile stress, showing obvious "quadratic stiffness." With the increase of steel content of SFCB tendon, the stiffness of beam is improved, the load-deflection curve begins to appear as a double-fold line characteristic compared with the normal FRP-reinforced beam
3. Under the high stress state, the relative slip between the SFCB bars and the concrete as well as between the steel core and the carbon fiber causes the SFCB bar tensile stress loss, which in turn reduces the ultimate bearing capacity of the SFCB bar-reinforced coral concrete beam; for rounded finish steel core, the bond performance between the carbon fibers and steel core is significantly weaker than that of the threaded steel core, and the steel core slip is more likely to occur under higher tensile stress.
4. When Using ACI440.1R-15 and GB50608-2010 to calculate the flexural capacity of the SFCB beams, the ratios of the theoretical value and the measured value from tests are 1.07 and 1.12, respectively. By introducing the two new factors k_1 and k_2, the calculation formula from ACI440.1R-15 and GB50608-2010 is modified to calculate the ultimate flexural capacity of SFCB reinforced concrete beam. The results show that the calculated result of the modified formula is closer to the experimental value, which can better reflect the actual stress state of SFCB bar coral concrete beam. It should be pointed out that this test is an exploratory test of the bending resistance of SFCB and coral concrete. The number of tests is relatively small. For the proposal to introduce k_1 and k_2 and their values, more test data are still needed to be checked.

ACKNOWLEDGMENTS

This article is supported by the National Natural Science Foundation of China (51868014), the High-Level Innovation Team in Colleges and Universities and Excellence Scholar Program "Island and Coastal Environment Concrete Structure "in Guangxi (201738-2) and Innovation-driven Development Project "Development and Demonstration of High-Erosion Construction Materials in Complex Marine Environment" in Guangxi (AA18242007-5). The views expressed are the authors' alone.

CONFLICT OF INTEREST

The authors declare that they have no known competing financial interests or personal relationships that could have appeared to influence the work reported in this paper.

DATA AVAILABILITY STATEMENT

The data used to support the findings of this study are available from the authors upon request.

ORCID

Feng Fu https://orcid.org/0000-0002-9176-8159

REFERENCES

1. Wang L, Zhao Y, Haibo LV. Prospect on the properties and application situation of coral aggregate concrete. Concrete. 2012;268(2):99–113. (in Chinese).
2. Gao Y, Wei Z, Sun X. Experimental research on basic mechanical properties of coral aggregate concrete. J Naval Eng University. 2017;29(01):64–68. (in Chinese).
3. Wang L, Fan L. Analysis of strength characteristics and failure modes of coral fragment concrete. China Concr Cem Prod. 2015;1(1):1–4. (in Chinese).

4. W. Yodsudjai, N. Otsuki, T. Nishida, et al. 2003. Study on strength and durability of concrete using low quality coarse aggregate from circurm-pacific region Paper presented at: Fourth Regional Symposium on Infrastructure Development in Civil Engineering (RSID4), pp. 171–180.
5. Wang L, Mao Y, Lv H, Chen S, Li W. Bond properties between FRP bars and coral concrete under seawater conditions at 30, 60, and 80 °C. Construct Build Mater. 2018;162: 442–449.
6. Ehlert RA, Holmes,Narver. Coral concrete at bikini atoll. Concr Int. 1991;13(1):19–24.
7. Dong Z, Gang WU, Hong ZHU. Mechanical properties of seawater sea-sand concrete reinforced with discrete BFRP-needles. Construct Build Mater. 2019;206(5):432–441.
8. Tomlinson D, Fam A. Performance of concrete beams reinforced with basalt FRP for flexure and shear. J Compos Constr. 2015;19(2):04014036.
9. Dong Z, Wu G, Zhao X, Ling J. Long-term bond durability of fiber-reinforced polymer bars embedded in seawater sea-sand concrete under ocean environments. J Compos Const. 2018;22 (10):0401814201–0401814212
10. Grace NF, Soliman AK, Abdel-Sayed G, Saleh KR. Behavior and ductility of simple and continuous FRP reinforced beams. J Compos Constr. 1998;2(4):186–194.
11. Kassem C, Farghaly AS, Benmokrane B. Evaluation of flexural behavior and serviceability performance of concrete beams reinforced with FRP bars. J Compos Constr. 2011;15(5): 682–695.
12. Elgabbas F, Vincent P, Ahmed EA, Benmokrane B. Experimental testing of basalt-fiber-reinforced polymer bars in concrete beams. Composites, Part B. 2016;91:205–218.
13. Tan, K. H. 1997. Behavior of hybrid FRP-steel reinforced concrete beams. Paper presented at Proceedings 3rd International Symposium on Non-Metallic (FRP) Reinforcement for Concrete Structures (FRPRCS-3)Japan Concrete Institute, Tokyo, 487–494.
14. Aiello MA, Ombres L. Structural performances of concrete beams with hybrid (fiber-reinforced polymer-steel) reinforcements. J Compos Constr. 2002;6:133–140. https://doi.org/10.1061/(ASCE)1090-0268(2002)6:2(133).
15. Lau D, Pam HJ. Experimental study of hybrid FRP reinforced concrete beams. Eng Struc. 2010;32(12):3857–3865.
16. Hao Q, Wang Y, Hou J, Ou J. Bond-slip constitutive model between GFRP/steel wire composite rebars and concrete. Eng Mech. 2009;26(05):62–72. (in Chinese).
17. Hao Q, Wang Y, Jinping O. Experimental study and design recommendation on concrete cover thickness of GFRP/steel wire composite rebars.Journal of architectural. Structure. 2009;30 (03):87–94. (in Chinese).
18. Wu G, Luo Y, Wu Z, Hu X, Zhang M. Experimental and theoretical studies on the mechanical properties of steel-FRP composite bars. Civil Eng J. 2010;43(03):53–61. (in Chinese).
19. Li Y, Wang Y, Ou J. Mechanical behavior of BFRP-steel composite plate under axial tension. Polymers. 2014;6(6): 1862–1876.
20. Sun Y, Qin WH, Ren ST, Wu G. Experimental study on flexural behavior of concrete beams reinforced by steel-FRP composite bars. J Reinforced Plast Compos. 2012;31(12): 1737–1745.
21. Dong Z, Wu G, Xu Y. Experimental study on the bond durability between steel-FRP composite bars (SFCBs) and sea sand concrete in ocean environment. Construct Build Mater. 2016;4 (6):277–284.
22. Wang L, Zhang J, Chen W, Fu F, Qian K. Short term crack width prediction of CFRP bars reinforced coral concrete. Eng Struct. 2020;218:110829.
23. Wang L, Zhang J, Huang C, Fu F. Comparative study of steel-FRP, FRP and steel-reinforced coral concrete beams in their flexural performance. Materials. 2020;13(9):2097–2097.
24. Wang L, Song Z, Yi J, Li J, Fu F, Qian K. Experimental studies on bond performance of BFRP bars reinforced coral aggregate concrete. Int J Concr Struct Mater. 2019;13(1):1–10.
25. ACI committee 440. Guide for the design and construction of structural concrete reinforced with Fiber-Reinforced Polymer (FRP) Bars. Farmington Hills: American Concrete Institute, 2015.
26. GB50608-2010. Technical code for infrastructure application of FRP composites. Beijing: China Planning Press, 2011 (in Chinese).
27. GB50010-2010. Code for design of concrete structures. Beijing: China Architecture & Building Press, 2011 (in Chinese).
28. JG12-2006. Light aggregate concrete structure design practice. Beijing. Beijing,China: China Planning Press, 2006 (in Chinese).
29. ACI committee 318. Building code Requirements for structural concrete (ACI318-14) and Commentary(318R-14) Farmington Hills:American Concrete Institute, 2014.
30. Fu F, Lam D, Ye J. Moment resistance and rotation capacity of semi-rigid composite connections with precast hollowcore slabs. J Constr Steel Res. 2010;66(3):452–461.
31. Gao S, LH Guo FF, Zhang SM. Capacity of semi-rigid composite joints in accommodating column loss. J Constr Steel Res. 2017;139(12):288–301.
32. Guo L, Liu Y, Fu F, Huang H. Behavior of axially loaded circular stainless steel tube confined concrete stub columns. Thin-Walled Struct. 2019;139(June 2019):66–76.
33. Deng XF, Liang SL, Fu F, Qian K. Effects of high-strength concrete on progressive collapse resistance of reinforced concrete frame. J Struct Eng. 2020;146(6):04020078.
34. Qian K, Liang SL, Xiong XY, Fu F, Fang Q. Quasi-static and dynamic behavior of precast concrete frames with high performance dry connections subjected to loss of a penultimate column scenario. Eng Struct. 2020;205:110115.
35. Weng YH, Qian K, Fu F, Fang Q. Numerical investigation on load redistribution capacity of flat slab substructures to resist progressive collapse. J Build Eng. 2020;29:101109.
36. Fu F. Response of a multi-storey steel composite building with concentric bracing under consecutive column removal scenarios. J Constr Steel Res. 2012;70:115–126.
37. Fu F, Lam D, Ye J. Modelling semi-rigid composite joints with precast hollowcore slabs in hogging moment region. J Constr Steel Res. 2008;64(12):1408–1419.
38. Wang L, Shen N, Zhang M, Fu F, Qian K. Bond performance of steel-CFRP bar reinforced coral concrete beams. Construct Build Mater. 2020;245:118456–118456.

AUTHOR BIOGRAPHIES

Lei Wang
Professor, College of Civil Engineering and Architecture
Guilin University of Technology
Guilin, China
wanglei@glut.edu.cn

Zhaoping Song
Research student, College of Civil Engineering and Architecture
Guilin University of Technology
Guilin, China
2315404461@qq.com

Changshi Huang
Research student, College of Civil Engineering and Architecture
Guilin University of Technology
Guilin, China
839098654@qq.com

Linjian Ma
Associate Professor, State Key Laboratory of Disaster Prevention and Mitigation of Explosion and Impact
Army Engineering University of PLA
Nanjing, China
patton.4400@163.com

Feng Fu
Senior Lecturer (Associate Professor) School of Mathematics, Computer Science and Engineering, City University of London, U.K
cenffu@yahoo.co.uk

How to cite this article: Wang L, Song Z, Huang C, Ma L, Fu F. Flexural capacity of steel-FCB bar-reinforced coral concrete beams. *Structural Concrete*. 2020;1–14. https://doi.org/10.1002/suco.201900409